LA-UR- 10-00954

Approved for public release; distribution is unlimited.

Title:	Plastic Instabilities in Statically and Dynamically Loaded Spherical Shells
Author(s):	T.A. Duffey E.A. Rodriguez
Intended for:	2010ASME Pressure Vessels and Piping (PVP) Conference Bellevue, WA July 18-22, 2010

Los Alamos
NATIONAL LABORATORY
EST.1943

Form 836 (7/06)

Proceedings of the ASME 2010 Pressure Vessels & Piping Division / K-PVP Conference
PVP2010
July 18-22, 2010, Bellevue, Washington, USA

DRAFT

PVP2010-25230

PLASTIC INSTABILITIES IN STATICALLY AND DYNAMICALLY LOADED SPHERICAL VESSELS

Thomas A. Duffey
Consulting Engineer
PO Box 1239
Tijeras, NM 87059 USA
505-281-1241
TDuffey2@aol.com

Edward A. Rodriguez
Global Nuclear network Analysis, LLC
PO Box 4850
Los Alamos, NM 87544 USA
505-672-9177
erodriguez@gnna.net

ABSTRACT

Significant changes were made in design limits for pressurized vessels in the 2007 version of the ASME Code (Section VIII, Div. 3) and 2008 and 2009 Addenda. There is now a local damage-mechanics based strain-exhaustion limit as well as the well-known global plastic collapse limit. Moreover, Code Case 2564 (Section VIII, Div. 3) has recently been approved to address impulsively loaded vessels.

It is the purpose of this paper to investigate the plastic collapse limit as it applies to dynamically loaded spherical vessels. Plastic instabilities that could potentially develop in spherical shells under symmetric loading conditions are examined for a variety of plastic constitutive relations. First, a literature survey of both static and dynamic instabilities associated with spherical shells is presented. Then, a general plastic instability condition for spherical shells subjected to displacement controlled and impulsive loading is given. This instability condition is evaluated for six plastic and visco-plastic constitutive relations. The role of strain-rate sensitivity on the instability point is investigated. Calculations for statically and dynamically loaded spherical shells are presented, illustrating the formation of instabilities as well as the role of imperfections. Conclusions of this work are that there are two fundamental *types* of instabilities associated with failure of spherical shells. In the case of impulsively loaded vessels, where the pulse duration is short compared to the fundamental period of the structure, one instability type is found not to occur in the absence of static internal pressure. Moreover, it is found that the specific role of strain-rate sensitivity on the instability strain depends on the form of the constitutive relation assumed.

1. INTRODUCTION

Design rules for impulsively loaded containment vessels have recently been accounted for in Section VIII, Division 3 (High Pressure Vessels) of the ASME Code through Code Case 2564.

Plastic tensile instability is one potential mechanism leading to global failure of pressure vessels. This instability is well known to occur for spherical pressure vessels subjected to static pressure loading, i.e., 'load control'. However, for conditions of 'displacement control', closely associated with the impulsive loading condition, less is known. For sudden impulsive pressure loading, the loading may be completed well before peak response of the vessel occurs.

A detailed discussion of earlier instability investigations [1-5] for spherical shells under static (load and displacement control) and pressure-pulse loading is presented in [6]. These investigations were almost exclusively limited to a plastic stress-strain law of the form

$$\bar{\sigma} = C\bar{\varepsilon}^{n} \tag{1}$$

where $\bar{\sigma}$ is equivalent true stress, $\bar{\varepsilon}$ is equivalent true strain, and C and n are material constants. The instability conditions and associated instability strains reported for static-pressure loading (load control), displacement (volume) control, and pressure-pulse loading generally differed among the various papers summarized in [6]. These differences in the instabilities would be anticipated, given that the instability behavior must be different for static-pressure loading when compared with short-duration impulsive pressure loading. In particular, the pressure would no longer be acting when peak response of an impulsively loaded vessel is reached. However, discrepancies between reported instability strains under displacement control were also noted in [6].

Updike and Kalnins [7] developed a numerical methodology for determining the plastic tensile instability limit for static pressure loading of axisymmetric vessels. They report that the plastic tensile instability limit (instability pressure) is an upper bound to actual burst test results. Hillier [8] addresses the difference between strains at instability and strains at fracture, which may account for some of the differences between calculations and experiments brought out by Updike and Kalnins [7]. A detailed investigation of plastic instability of static-pressure-

loaded vessels is presented by Mou, et al. [9], where it is shown that there exist two types of instabilities: Global and Local. Results are illustrated for both cylindrical and spherical shells. Global plastic instability (also termed 'structural instability') occurs when the (monotonically increasing) pressure reaches a maximum in the vessel; whereas local plastic instability (termed 'material instability') is related to the type of instability that occurs in the tension test where the increase in resistance due to strain hardening is just balanced by the decrease in area due to thinning of the specimen. Explicit solutions are presented in [9] for a bilinear stress-strain curve.

In cases where the shell is loaded by a dynamic internal pressure pulse with duration on the order of or greater than the vessel response time, Tugcu [10] terms the global plastic instability as a *dynamic instability with respect to time*.

Needleman [11] investigates the bifurcation of elastic-plastic spherical shells subjected to static loading, using a variational principle attributed to Hill. Two cases are considered in [11]: prescribed internal pressure; and prescribed change in volume enclosed by the shell. These appear to be equivalent to 'load' and 'displacement' control, respectively. Needleman considers axisymmetric bifurcations, i.e., those that vary only with the meridional coordinate φ (see Fig. 1), and introduces a complete set of bifurcation modes using Legendre polynomials. It is found that the admissible functions for the two cases differ: The mode q=0 is admissible for prescribed internal pressure but is not admissible for the case of prescribed change in volume. However, q=1 is admissible in both cases: This mode corresponds to thinning at one pole with a corresponding thickening at the other, which seems to be related to necking localization. Had nonaxisymmetric modes been considered as well in [11], it is likely that the bifurcation mode would have appeared more aligned with necking localization. Summarizing, for static pressure loading, there is an instability in the fundamental mode, q=0, and a bifurcation at larger displacement in the q=1 mode. For a volume-prescribed change, only the bifurcation in the q=1 mode occurs. These results are in qualitative accord with Mou, et al. [9], using a different methodology. For pressure loading, the instability in the q=0 mode corresponds to the global or "structural" instability of Mou, et al. [8], whereas the bifurcation in the q=1 mode is analogous to the local or "material" instability in [9].

A general instability condition for an impulsively loaded spherical shell is presented in Section 2 for several constitutive models. Finite element calculations for statically and dynamically loaded spherical shells and comparisons with the numerical results of others are presented in Section 3. Conclusions for this paper are summarized in Section 4. Dynamic effects anticipated at higher loading rates are discussed in the Appendix.

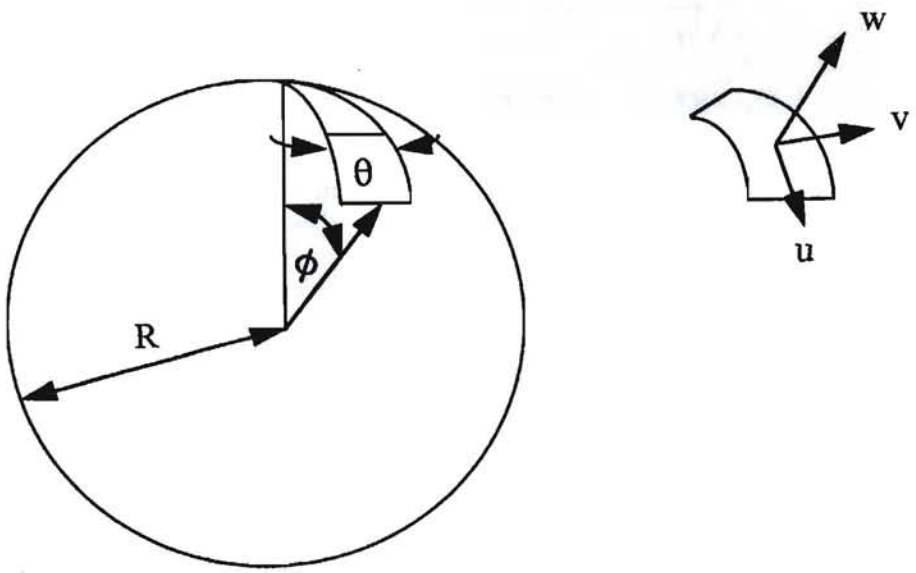

Figure 1. Coordinates of Spherical Shell

NOMENCLATURE

A_0	original area of shell cross section
C, n	power law material constants
D,m	strain-rate material constants
N_θ	normal force
p	internal pressure
q	axisymmetric mode number
r	current radius
r_0	original radius
t	current thickness
t_0	original thickness
$\bar{\varepsilon}$	equivalent true strain
ε_i	i^{th} true strain component
$\varepsilon_{eng\,i}$	i^{th} engineering strain component
ρ	mass density
$\bar{\sigma}$	equivalent true stress

σ_i	i^{th} true stress component
σ_{eng_i}	i^{th} engineering stress component
σ_0, K	generalized power law material constants
Φ	meridional coordinate
$(\,)^*$	denotes instability point

2. CALCULATION OF INSTABILITIES FOR A SPHERICAL SHELL

As derived by Cooper [1], the instability for a spherical shell subjected to displacement-controlled or impulsive loading is analogous to the plastic tensile instability that occurs in a uniaxially loaded tensile specimen. This type of instability would occur when the force exerted by one hemisphere upon the other reaches a maximum. This instability would be followed by localized deformation (necking) of the shell. Cooper [1] determines that this instability occurs at a hoop strain of $\frac{1}{2}(n+1)$ for the plastic stress-strain relation shown in Eqn. (1). As shown in [6] this instability strain is in fact much lower (n). A similar result has been reported for cylindrical shells (with experimental corroboration) by Nakamura, et al. [4]. A general expression for this instability condition for a spherical shell along with the equations leading up to the expression are needed in developing the results in this paper. The previously developed derivation from [1,6] is as follows:

Consider one half of a free, thin spherical shell. The hemisphere is assumed loaded by some displacement-controlled mechanism, such as the impulsive velocity from some earlier transient pressure pulse loading. The total force (normal force, N_θ) imparted by one hemisphere upon the other is

$$N_\theta = 2\pi r t \sigma_\theta \tag{2}$$

where r is the current radius, t is the current thickness and σ_θ is the true in-plane stress normal to the cut surface. This normal force is a maximum when its derivative is set to zero. Noting that r, t, and σ_θ are variables, the differential of the normal force becomes

$$d(N_\theta) = 2\pi t \sigma_\theta dr + 2\pi r \sigma_\theta dt + 2\pi r t d\sigma_\theta \equiv 0 \tag{3}$$

or

$$\frac{dr}{r} + \frac{dt}{t} + \frac{d\sigma_\theta}{\sigma_\theta} = 0 \tag{4}$$

True strains for this uniformly expanding spherical shell are

$$\varepsilon_r = \ln\left(\frac{t}{t_0}\right)$$
$$\varepsilon_\theta = \varepsilon_\phi = \ln\left(\frac{r}{r_0}\right) \tag{5}$$

where t_0 and r_0 denote initial thickness and radius, respectively.

Corresponding differential strains are

$$d\varepsilon_r = \frac{dt}{t}$$
$$d\varepsilon_\theta = d\varepsilon_\phi = \frac{dr}{r} \tag{6}$$

Assuming incompressibility of plastic strains,

$$\varepsilon_\theta + \varepsilon_\phi + \varepsilon_r = 0$$
$$\varepsilon_r = -2\varepsilon_\theta \tag{7}$$
$$d\varepsilon_r = -2d\varepsilon_\theta$$

Substituting appropriate expressions from Equations (5)-(7) into Equation (4) results in

$$\sigma_\theta = \frac{d\sigma_\theta}{d\varepsilon_\theta} \tag{8}$$

Equivalent strain, $\bar{\varepsilon}$, is defined as

$$\left[\frac{3}{\sqrt{2}}\bar{\varepsilon}\right]^2 = (\varepsilon_x - \varepsilon_y)^2 + (\varepsilon_y - \varepsilon_z)^2 + (\varepsilon_z - \varepsilon_x)^2 \tag{9}$$

Let

$$\varepsilon_x = \varepsilon_\theta$$
$$\varepsilon_y = \varepsilon_\phi \tag{10}$$
$$\varepsilon_z = \varepsilon_r$$

Substituting Equations (7) and (10) into Equation (9) results in

$$\bar{\varepsilon} = 2\varepsilon_\theta \tag{11}$$

Equivalent Stress, $\bar{\sigma}$, is defined as

$$2\bar{\sigma}^2 = (\sigma_x - \sigma_y)^2 + (\sigma_y - \sigma_z)^2 + (\sigma_z - \sigma_x)^2 \tag{12}$$

Let

$$\sigma_x = \sigma_\theta$$
$$\sigma_y = \sigma_\phi \quad (13)$$
$$\sigma_z = \sigma_r$$

But

$$\sigma_\theta = \sigma_\phi \text{ and} \quad (14)$$

$$\sigma_r = 0 .$$

Combining Equations (12)-(14) results in

$$\overline{\sigma} = \sigma_\theta \quad (15)$$

Now from Equation (11),

$$d\varepsilon_\theta = d\overline{\varepsilon}/2 \quad (16)$$

and from Equation (15),

$$d\sigma_\theta = d\overline{\sigma} \quad (17)$$

Combining Equations (8) and (15)-(17),

$$\frac{d\overline{\sigma}}{d\overline{\varepsilon}} = \frac{\overline{\sigma}}{2} \quad (18)$$

Eqn. (18) is the needed expression from [1,6]. At this point, the stress-strain curve is yet to be specified. Six cases are considered as follows:

2.1 Power Law: Assume an equivalent stress-equivalent strain curve of the form given by Equation (1). Substituting Equation (1) into (18), it is straightforward to show that

$$n = \frac{\overline{\varepsilon}^*}{2} \quad (19)$$

where the * denotes the instability point. From Equation (11),

$$\varepsilon_\theta^* = n \quad (20)$$

Therefore, the instability for a complete spherical shell under impulsive load occurs when the circumferential strain is equal to the strain at necking in the tensile test. This is the same result as obtained in the case of the cylindrical shell by Nakamura, et al. [4].

This instability is of a different nature than that associated with reaching maximum pressure. The instability associated with attaining maximum pressure is a *global* or *structural* instability, utilizing the terminology introduced by Mou, et al. [9]. On the other hand, the instability associated with maximizing the normal force is *local* or *material* in nature. In fact, the global instability (for a cylinder and a sphere) will *not* occur for impulsively loaded vessels in the absence of internal pressurization, whereas the local instability does not depend upon a pressure load being present.

Finally, inertial effects may well influence the initiation and growth of local instabilities, such as necking.

2.2 Generalized Power Law: Now assume an equivalent stress-strain curve of the form,

$$\overline{\sigma} = \sigma_0 + K\overline{\varepsilon}^n \quad (21)$$

Then, using Eqns. (11), (15), and (18), it is straightforward to show that the instability strain, ε_θ^*, is given by the following transcendental equation:

$$(2\varepsilon_\theta^*)^n \left[\frac{n}{\varepsilon_\theta^*} - 1\right] = \frac{\sigma_0}{K} \quad (22)$$

2.3 Bilinear Form: For a bilinear stress-strain curve (n=1), Eqn. (22) reduces to

$$\varepsilon_\theta^* = 1 - \frac{\sigma_0}{2K} \quad (23)$$

2.4 Generalized Power Law Including Strain Rate Sensitivity: Strain rate sensitivity can be included by adding a power-law term with exponent, m, similar to the work-hardening exponent, n. This strain-rate sensitivity term is described by Keeler [12] and Boyce, et al [13]. Adding this term to Eqn. (21) results in

$$\overline{\sigma} = \sigma_0 + K\overline{\varepsilon}^n + D\dot{\overline{\varepsilon}}^m \quad (24)$$

where D is a constant and $\dot{\overline{\varepsilon}}$ denotes equivalent true strain rate. Using Eqns. (11), (15), and (18), the instability strain is given by the following transcendental equation:

$$(2\varepsilon_\theta^*)^n \left[\frac{n}{\varepsilon_\theta^*} - 1\right] = \frac{\sigma_0 + D(2\dot{\varepsilon}_\theta)^m}{K} \quad (25)$$

As an example, from Keeler [12], for AKDQ steel, typical values of exponents are n=+0.21 and m=+0.012. Boyce, et al [13] report a range in m-values of 0.004-0.007 for four high-strength, high-toughness steels, but state that these values are quite low compared to most metals, which fall in the range of m = 0.02-0.2, based on Ref. [14].

2.5 Bilinear Hardening with Strain Rate Sensitivity: For bilinear strain hardening (n=1) and power-law strain rate sensitivity, Eqn. (25) reduces to:

$$\varepsilon_\theta^* = 1 - \frac{\sigma_0}{2K} - \frac{D}{2K}(2\dot{\varepsilon}_\theta)^m \tag{26}$$

The instability strain therefore depends on the current strain rate. Eqn. (26) reduces to Eqn. (23) in the absence of strain rate sensitivity. Note that the instability strain decreases (for positive m), in agreement with Refs. [13] and [14], but apparently not with [12]. Keeler [12] states that a positive m-value retards the growth of the incipient neck, implying an increase in ductility.

2.6 Product-Type Bilinear Hardening and Linear Strain Rate Sensitivity: The commonly used Johnson-Cook constitutive relation utilizes a product-type law, where the strain-hardening term is multiplied with the strain-rate term. The following simplified stress-strain relationship, with bilinear strain hardening and linear strain rate sensitivity, has this type of attribute:

$$\bar{\sigma} = \left[A + B\bar{\varepsilon}\right]\left[1 + C\dot{\bar{\varepsilon}}\right] \tag{27}$$

where A, B, and C are constants. Utilizing Eqns. (11), (15), and (18), the instability strain, ε_θ^*, is:

$$\varepsilon_\theta^* = 1 - \frac{A}{2B} \tag{28}$$

This result is the same as for bilinear strain hardening without strain rate sensitivity (Eqn. (22)). Therefore, strain rate sensitivity does not influence the instability strain for this form of stress-strain relationship.

3. NUMERICAL INVESTIGATION

3.1 Finite Element Calculation results on Instabilities for Spherical Shells will be placed here by Edward Rodriguez.

3.2 Comparisons with Mou, et al. [9]: Mou, et al. [9] present 'structural' and 'material' instability strain results for a bilinear stress-strain curve, including a numerical example for a spherical shell. This same numerical example is utilized here to investigate instabilities of a spherical shell.

From Eqn. (21), using n = 1 (bilinear stress-strain curve), the true stress, true strain relationship becomes

$$\bar{\sigma} = \sigma_0 + K\bar{\varepsilon} \tag{29}$$

As shown in Eqns. (15) and (11), the equivalent true stress and strain are related to the principal true stress and strain components by

$$\bar{\sigma} = \sigma_\theta \text{ and } \bar{\varepsilon} = 2\varepsilon_\theta \tag{30}$$

Noting that the engineering hoop stress, σ_{eng_θ}, and strain, ε_{eng_θ}, are related to the corresponding true stress, σ_θ, and true strain, ε_θ through

$$\begin{aligned} \sigma_\theta &= \sigma_{eng_\theta}(1 + \varepsilon_{eng_\theta}) \\ \varepsilon_\theta &= \ln(1 + \varepsilon_{eng_\theta}) \end{aligned} \tag{31}$$

then Eqn (29) can be written

$$\sigma_{eng_\theta} = \frac{\sigma_0 + 2K\ln(1 + \varepsilon_{eng_\theta})}{1 + \varepsilon_{eng_\theta}} \tag{32}$$

The normal force acting over one half the spherical shell (see Eqn. (2)) can be written $N_\theta = \sigma_{eng_\theta} A_0$, where A_0 is the original area of the shell cross section. This normal force in the spherical shell can be expressed in the nondimensional form suggested by Mou, et al. [9] as $\overline{F} = \frac{N_\theta}{KA_0}$. For the spherical shell, this can be written in terms of engineering hoop strain as:

$$\frac{N_\theta}{KA_0} = \frac{\sigma_0/K + 2\ln(1 + \varepsilon_{eng_\theta})}{1 + \varepsilon_{eng_\theta}} \tag{33}$$

A related expression can be developed for pressure in the spherical shell as a function of engineering hoop strain. First, it is noted that equilibrium requires

$$\sigma_\theta = \frac{pr}{2t} \tag{34}$$

where p is applied internal pressure, r is current radius and t is current thickness.
Solving Eqn. (34) in terms of pressure and substituting the bilinear stress-strain relation,

$$p = \frac{2t}{r}\left[\sigma_0 + 2K\varepsilon_\theta\right] \tag{35}$$

where ε_θ is the true hoop strain. Using Eqn. (31), Eqn. (35) can be written as

$$\frac{p}{K\left(\frac{t_0}{r_0}\right)} = 2\left(\frac{t}{t_0}\right)\left(\frac{r_0}{r}\right)\left[\frac{\sigma_0}{K} + 2\ln(1 + \varepsilon_{eng_\theta})\right] \tag{36}$$

Constancy of volume in the plastic range requires that

$$4\pi r_0^2 t_0 = 4\pi r^2 t \tag{37}$$

Utilizing Eqn. (37) with (36) results in

$$\frac{p}{K\left(\frac{t_0}{r_0}\right)} = 2\left(\frac{r_0}{r}\right)^3\left[\frac{\sigma_0}{K} + 2\ln(1+\varepsilon_{eng_\theta})\right] \qquad (38)$$

Noting that

$$\frac{r}{r_0} = \frac{(r_0+\delta)}{r_0} = 1+\varepsilon_{eng_\theta} \qquad (39)$$

then Eqn. (38) becomes

$$\frac{p}{K\left(\frac{t_0}{r_0}\right)} = \frac{2}{(1+\varepsilon_{eng_\theta})^3}\left[\frac{\sigma_0}{K} + 2\ln(1+\varepsilon_{eng_\theta})\right] \qquad (40)$$

Equations (33) and (40) are plotted in Figure 2 as a function of engineering hoop strain for $\sigma_0 / K = 0.1$. The peak of each curve corresponds to the respective instability point. Structural instability is seen to occur at an engineering hoop strain of 0.33 in/in. Material instability occurs at an engineering hoop strain of 1.59 in/in. These curves can be directly compared to corresponding curves for a similar cylindrical shell example developed in Reference [9].

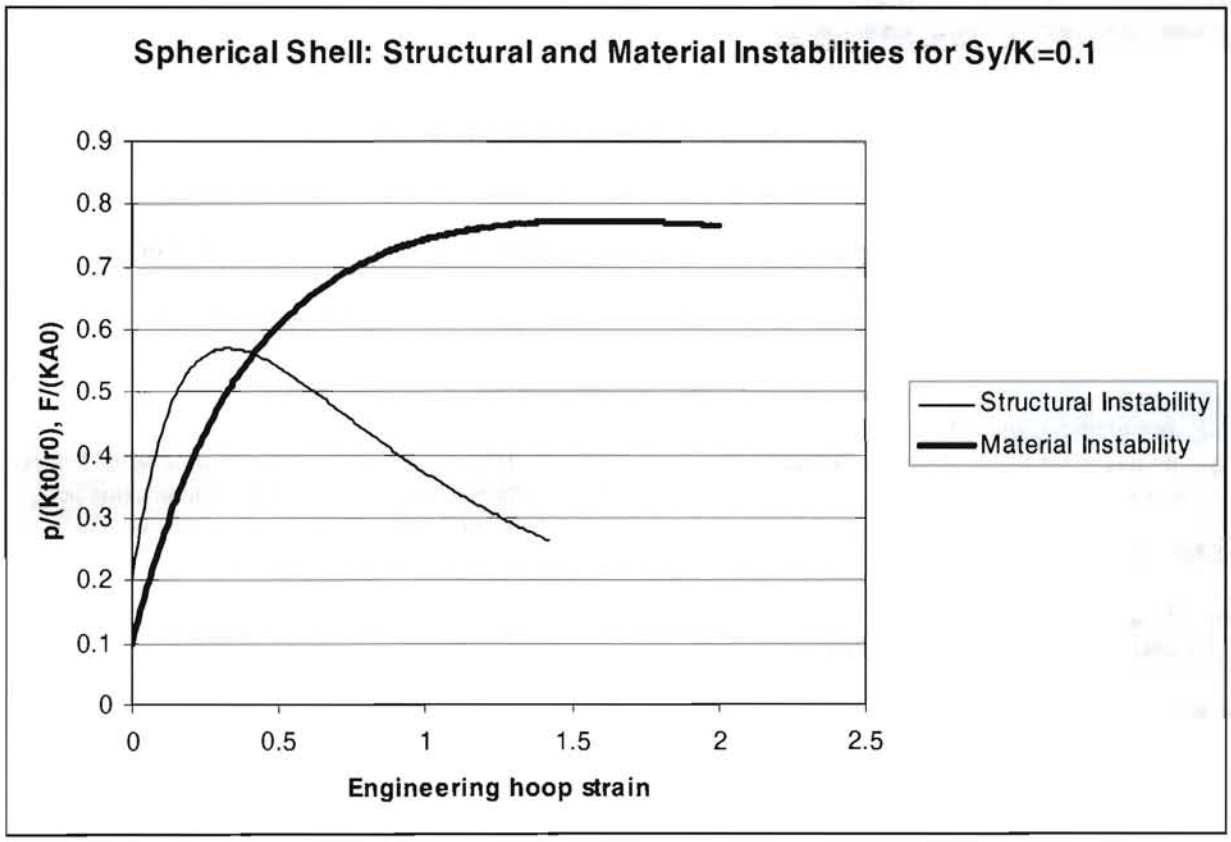

Figure 2. Structural and material instabilities for a spherical shell with bilinear stress-strain relation and $\sigma_0 / K = 0.1$

Results for the spherical shell numerical example in Mou, et al. [9] are shown in Fig. 3 (inside radius 100 in; thickness 1 in; $\sigma_0 = 30ksi$; K = 60 ksi), with the instability true hoop strain of 0.751 (. This is the 'material' instability described by Mou, et al. This result agrees with Eqn. (3.12) of Mou, et al [9], but not with the reported value of 0.50 strain in Section 4.3 of [9]. The corresponding plot of internal pressure as a function of radial displacement, showing the 'structural' instability for this numerical example, is plotted as Fig. 4.3-2 in Mou, et al. [9] and is not repeated here. The structural instability occurs at an engineering hoop strain of 0.0833 in/in.

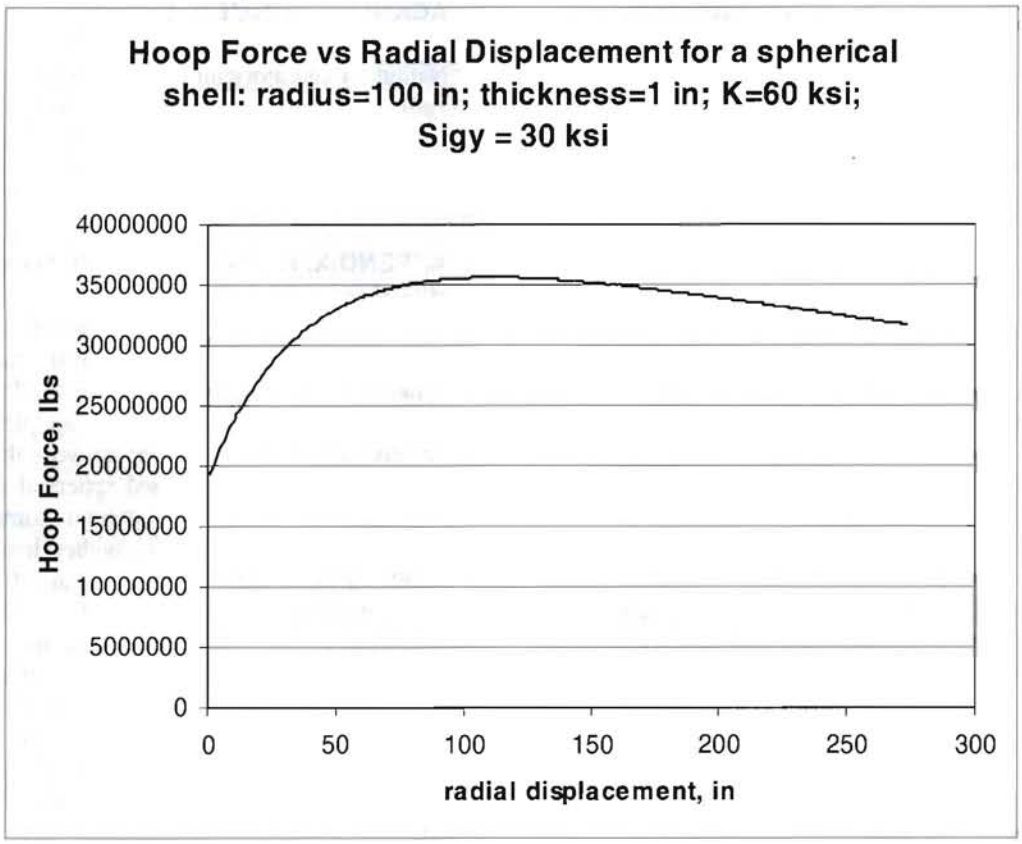

Figure 3. Hoop force as a function of radial displacement for example problem utilized in Mou, et al. [9]

4. RESULTS AND CONCLUSIONS

There are two types of instabilities that are observed for spherical shells, and they are categorized as either "global (structural)" or "local (material)" in nature, using nomenclature introduced by Mou, et al. [9]. In the case of a "global" instability, the shell radially expands, accelerating in uncontrolled manner by excess pressure loading, but deformations do not necessarily localize. This type of instability is associated with static internal pressure loading and occurs when the internal pressure reaches a maximum, i.e., dp=0. In this case, the increase in stress due to strain hardening is insufficient to overcome the decrease in carrying capacity due to shell thinning and increase in radius. It does not occur in the case of purely impulsive loading in the absence of a finite-duration pressure pulse.

The second type of instability, termed here "local" instability, leads to necking-type localization. It is the stress resultant, N, that reaches a maximum for this type of instability, i.e., dN=0. This local instability is associated with both pressurized shells and impulsively loaded shells, and manifests itself in the formation of local necking of the cross section. This local instability is the subject of the present paper. Utilizing a general instability expression for spherical shells under displacement (volume) control or impulsive loading, strain expressions at the point of instability are developed for a variety of plastic stress-strain relationships. The effect of strain-rate sensitivity is also incorporated and its importance is found to depend upon the specific viscoplastic stress-strain relationship.

These results have implications regarding Section VIII, Division 3 of the ASME Code and associated Code Case 2564. Both have two general limit criteria for ductile elastic-plastic behavior: A global, plastic-instability collapse limit and local strain-exhaustion limits. It appears that, in the case of impulsively loaded vessels, the global plastic-instability collapse limit would not occur in the absence of static pressure loading. The local (material) failure would be accounted for in the strain-exhaustion limits.

REFERENCES

[1] Cooper, W.E., 1957, "The Significance of the Tensile Test to Pressure Vessel Design", Welding Research Supplement, pp. 49s – 56s.

[2] Cooper, W.E., 1981, "Rationale for a Standard on the Requalification of Nuclear Class 1 Pressure-Boundary Components", Report EPRI NP-1921, Electric Power Research Institute, Palo Alto, CA.

[3] Mellor, P.B., 1960, "The Ultimate Strength of Thin-Walled Shells and Circular Diaphragms Subjected to Hydrostatic Pressure", International Journal of Mechanical Sciences, 1, pp. 216-228.

[4] Nakamura, T., Kaguchi, H., and Kubo, S., 2000, "Failure Strain of Thin Cylindrical Vessel Subjected to Dynamic Internal Pressure", Design and Analysis of Pressure Vessels and Piping-2000, R. Baliga, Ed., PVP-Vol 399, pp. 47-54.

[5] Hillier, M.J., 1966, "The Inertia Effect in the Tensile Plastic Instability of a Thin Spherical Shell", International Journal of Mechanical Sciences, 8, pp. 61-62.

[6] Duffey, T.A., and Doyle, D., 2006, "Plastic Instabilities in Spherical Shells Under Load, Displacement, and Impulsive Loading", 2006, Proceedings of PVP2006-IPVT-11, Paper 93727, Vancouver, BC, Canada
[7] Updike, D.P., and Kalnins, A., 1998, "Tensile Plastic Instability of Axisymmetric Pressure Vessels", Journal of Pressure Vessel Technology, 120, pp. 6-11.
[8] Hillier, M.J., 1965, "Tensile Plastic Instability of Thin Tubes-II", International Journal of Mechanical Sciences, 7, pp. 539-549.
[9] Y. Mou, W.D. Reinhardt, R.K. Kizhatil and G.H. McClellan, 1998, "Plastic Instability in Pressure Vessels and their Role in Design", PVP-V0l. 370, Finite Element Applications: Linear, Non-Linear, Optimization and Fatigue and Fracture, ASME, pp. 135-141.
[10] Tugcu, 2003,"Instability and ductile failure of thin cylindrical tubes under internal pressure impact", International Journal of Impact Engineering, 28, pp. 183-205.
[11] A. Needleman,1975, "Bifurcation of Elastic-Plastic Spherical Shells Subject to Internal Pressure", Journal of the Mechanics and Physics of Solids, Vol. 23, pp. 357-367.
[12] S. Keeler, January 2006, "How Forming Speed Affects Stretchability", MetalForming, pp. 56-57.
[13] B.L. Boyce, T.B. Crenshaw, and M.F. Dilmore, January 2007, "The Strain-Rate Sensitivity of High-Strength High-Toughness Steels", SAND2007-0036, Sandia National Laboratories, Albuquerque, NM.
[14] R.W. Hertzberg, 1989, *Deformation and Fracture Mechanics of Engineering Materials*, Third Edition, Wiley, New York.
[15] Faupel, J.H., 1964, Engineering Design, John Wiley and Sons, Inc., p. 385.
[16] Mercier, S., and Molinari, A., 2004, "Analysis of Multiple Necking in Rings Under Rapid Radial Expansion", International Journal of Impact Engineering, 30, pp. 403-419.
[17] Sorensen, N.J., and Freund, L.B., 2000, "Unstable Neck Formation in a Ductile Ring Subjected to Impulsive Radial Loading", International Journal of Solids and Structures, 37, pp. 2265-2283.
[18] Tuğcu, P., 2003, "Instability and Ductile Failure of Thin Cylindrical Tubes Under Internal Pressure Impact", International Journal of Impact Engineering, 28, pp. 183-205.
[19] Schreyer, H.L., and Chen, Z., 1986, "One-Dimensional Softening with Localization", Journal of Applied Mechanics, 53, pp. 791-797.
[20] Needleman, A., 1988, "Material Rate Dependence and Mesh Sensitivity in Localization Problems", Computer Methods in Applied Mechanics and Engineering, Vol. 67, pp. 69-85.
[21] Han, J. and Tvergaard, V., 1995, "Effects of Inertia on the Necking Behavior of Ring Specimens Under Rapid Radial Expension", European Journal of Mechanics A/Solids, Vol. 12, pp. 287-307.
[22] Guduru, P.R. and Freund, L.B., 2002, "The Dynamics of Multiple Neck Formation and Fragmentation in High Rate Extension of Ductile Materials", International Journal of Solids and Structures, Vol 39, pp. 5615-5632.
[23] Grady, D.E. and Benson, D.A., 1983, "Fragmentation of Metal Rings by Electromagnetic Loading", Experimental Mechanics, Vol. 12, pp 393-400.

ACKNOWLEDGMENTS

This work was supported by Group W-14, Los Alamos National Laboratory under Subcontract No. 71100-001-09, with Paul O. Leslie as Technical Monitor. The first author also wishes to thank Dr. H.L. Schreyer, Professor Emeritus, University of New Mexico, for valuable discussions on instabilities.

APPENDIX: A DISCUSSION OF DYNAMIC EFFECTS AT HIGHER LOADING RATES

Over the past decade, a number of papers [16-18] have been written regarding numerical analyses of failure in dynamically loaded rings, although the loading levels appear to be beyond those of interest for incipient failure of pressure vessels. There are similarities between the dynamic response of impulsively loaded rings and spherical shells, and it is likely that spherical shells will exhibit some of the phenomena observed for rings at these higher loading rates. Therefore, results of these numerical studies are discussed below. In all cases examined, the governing equations are sufficiently complicated that closed form solutions are not possible. The finite element numerical solutions are run for specific cases only, so it is difficult to see the role of the individual parameters on the formation of instabilities. Also in some cases finite element size plays a role in the predicted localization, influencing the results (Schreyer and Chen [19], Needleman [20]).

The rings in [16-18] are driven radially outward by sudden, impulsive loading. Failure by local necking is described. While quasi-static studies of ring expansion allude to the formation of a unique neck in the absence of inertia, these recent papers imply that for rings without any imperfection, necking is not observed. Dynamic necking apparently has to be triggered by small imperfections. The introduction of imperfections is required to initiate localization, although necking may or may not occur at imperfection sites [17]. Mercier and Molinari [16] also found that for dynamic cases, the instabilities introduced are not necessarily located at the sites at which unstable growth developed.

Han and Tvergaard [21] investigate dynamic necking behavior for impulsively loaded, strain-rate-independent rings. They show that wave propagation is an important parameter associated with multiple neck formation. Guduru and Freund [22] investigate the closely related problem of a cylindrical rod. They predict an increase in the number of necks and an increase in the bifurcation strain with increasing extension rate.

Grady and Benson [23] observe from experiments that the fracture strain is an increasing function of expansion speed of the ring. Thus, it has generally been found that average ductility of the rings increases with increasing initial impulse (or equivalently, velocity) and that the number of unstable necks that form increases with impulse level. However, the observed increase in apparent ductility with impulse level may well be associated with the increased numbers of necks formed at the higher loading levels.

It should be emphasized, however, that much of the work on dynamic loading and fragmentation of rings, e.g., the work of Grady and Benson [23] discussed above, was performed at strain rates well beyond those of interest in this

paper, which is focused on impulse levels leading to incipient failure, not on full fragmentation of the vessel.